Research Square

Preprints are preliminary reports that have not undergone peer review.
They should not be considered conclusive, used to inform clinical practice,
or referenced by the media as validated information.

Triptonide induces apoptosis and inhibits the proliferation of ovarian cancer cells by activating the p38/p53 pathway and autophagy

Ruoxuan Lou
Basic Medical College of Jinan University
Taohua Yang
First Affiliated Hospital of Jinan University
Xiaoying Zhang
Central Hospital of Panyu District
Jianyi Gu
Basic Medical College of Jinan University
Jiadai XueLu
First Affiliated Hospital of Jinan University
Danhui Gan
First Affiliated Hospital of Jinan University
Haijing Li
The Sixth Affiliated Hospital of Jinan University, Dongguan Eastern Central Hospital
Yuanhong Chen
The Sixth Affiliated Hospital of Jinan University, Dongguan Eastern Central Hospital
Jianwei Jiang
jjw703@jnu.edu.cn

Basic Medical College of Jinan University

Research Article

Keywords: Ovarian cancer, Apoptosis, Autophagy, Antitumor

Posted Date: February 20th, 2024

DOI: https://doi.org/10.21203/rs.3.rs-3946044/v1

License: This work is licensed under a Creative Commons Attribution 4.0 International License.
Read Full License

Additional Declarations: No competing interests reported.

Version of Record: A version of this preprint was published at Bioorganic & Medicinal Chemistry on June 1st, 2024. See the published version at https://doi.org/10.1016/j.bmc.2024.117788.

Abstract

Ovarian cancer is a common malignant tumor in women, and 70% of ovarian cancer patients are diagnosed at an advanced stage. Drug chemotherapy is an important method for treating ovarian cancer, but recurrence and chemotherapy resistance often lead to treatment failure. In this study, we screened 10 extracts of *Tripterygium wilfordii*, a traditional Chinese herb, and found that triptonide had potent anti-ovarian cancer activity and an IC50 of only 2.972 nM against A2780 cell lines. In addition, we determined that triptonide had a better antitumor effect on A2780 cell lines than platinum chemotherapeutic agents in vitro and that triptonide had no significant side effects in vivo. Further studies showed that triptonide exerts its anti-ovarian cancer effect through activation of the p38/p53 pathway and induction of autophagy to promote apoptosis, which provides a new candidate drug and strategy for the treatment of ovarian cancer.

1. Introduction

Ovarian cancer is the seventh most common cancer in women worldwide. Among women older than 40 years, ovarian cancer is the second most common malignant tumor after breast cancer and ranks as the fifth most common cause of cancer-related death in women [1]. There are three main types of ovarian cancer: epithelial (the most common), germ cell, and sex cord-stromal, with the latter two accounting for only approximately 5% of all ovarian cancers. However, due to asymptomatic development, 70% of ovarian cancer cases are diagnosed at an advanced stage. Despite years of research, there is still a lack of reliable diagnostic markers and other diagnostic methods that can be used for early detection and screening. Although ovarian cancer usually responds well to first-line chemotherapy comprising platinum compounds and taxanes, most patients develop recurrence and chemotherapy resistance, and the five-year survival rate is only approximately 30% [2–3]. Therefore, it is necessary to identify a therapeutic method to address the treatment dilemma of ovarian cancer.

The purification of drug monomers with good antitumor effects and few side effects from traditional Chinese herbs is a promising method for cancer treatment [4–5]. Triptonide is a diterpene compound extracted from the traditional Chinese medicine herb *Tripterygium wilfordii* that has pharmacological effects, such as anti-inflammatory effects, immunosuppression, and inhibition of tumorigenesis and angiogenesis, and is a promising antitumor drug monomer [6–9]. Previous studies have reported that triptonide does not cause serious side effects or toxicity to the liver in animal models [10–11].

The tumor suppressor p53 plays an important role in cellular responses to various stress signals, such as DNA damage, hypoxia, and oncogenic activation [12]. Activation of p53 can induce a range of responses, including cell cycle arrest, DNA repair, cell apoptosis and senescence, and it also acts as a tumor suppressor by preventing genomic damage or eliminating potentially oncogenic cells [13]. TP53 is the most frequently mutated gene in human cancers and is a hallmark of most human cancers. Approximately 50% of invasive tumors have p53 mutations, leading to significant defects in p53 function. In some refractory cancers, such as high-grade serous ovarian cancer, triple-negative breast cancer,

esophageal cancer, small cell lung cancer and squamous cell lung cancer, *TP53* can have a mutation rate higher than 80% [14]. Thus, p53 is an important candidate target for anticancer therapy strategies.

In this study, we screened 10 traditional Chinese medicine monomer compounds for their anti-ovarian cancer effects, and the results showed that among the various *Tripterygium wilfordii* monomers, ovarian cancer cells were the most sensitive to triptonide. We found that triptonide effectively inhibited the growth of ovarian cancer A2780 cells in vitro, induced apoptosis, and promoted S-phase arrest through activation of the p38/p53 pathway and the induction of lethal autophagy. Moreover, triptonide effectively inhibited tumor growth in xenograft mice. These data suggest that triptonide is a potential antitumor agent for the treatment of ovarian cancer.

2. Materials and Methods

2.1. Materials

Triptonide, tripterifordin, wilforgine, wilforine, oryhosphenic acid, triptophenolide, wilforlide A, triptolide, celastrol and demethylzeylasteral were obtained from Chengdu Must Biotech, Ltd, with a purity > 98%. Triptonide was dissolved in dimethyl sulfoxide (DMSO) for in vitro studies or in normal saline for in vivo experiments. Bafilomycin A1 and a p38 MAPK inhibitor (SB203580) were purchased from MCE (Shanghai, China) and dissolved in DMSO. Primary antibodies against p53, phospho-p53, p38, phospho-p38, cleaved PARP, GAPDH, CDK2, CDC25A, cyclin A, LC3, p62/SQSTM1, Beclin1 and others were purchased from Cell Signaling Technology (Boston, MA). The secondary antibodies goat anti-rabbit IgG-HRP and goat anti-mouse IgG-HRP were purchased from Santa Cruz Biotechnology (Santa Cruz, CA).

2.2. Cells and cell culture

The human ovarian cancer cell Line A2780 was obtained from Sunncell Biotechnology (Wuhan, China). The cells were maintained in RPMI-1640 medium supplemented with 10% FBS and 1% penicillin–streptomycin (KeyGEN, Jiangsu, China). The cells were cultured at 37°C in an atmosphere containing 5% CO_2.

2.3. Cell viability assay

The cells were seeded into 96-well plates at 3× 10^3 cells/well. After 24 h, the cells were incubated with different concentrations of triptonide (0, 4, 8, 16, 32 or 64 nM) for 48 h. Then, 20 μL of MTT solution (5 mg/mL) (Beyotime Biotechnology Shanghai, China) was added to each well, and the plates were incubated for another 4 h at 37°C before the optical density was measured at 570 nm by a microplate reader (Bio-Rad Laboratories, Hercules, CA, USA).

2.4. Colony formation assay

A2780 cells were seeded in six-well plates at a density of 500–800 cells/well, allowed to attach for 24 h, and subsequently exposed to different concentrations of triptonide (0, 0.25 and 0.5 nM) for 7–14 days.

The cells were fixed with 4% paraformaldehyde for 20 min and subsequently stained with 0.5% crystal violet solution for 30 mins. The stained colonies were counted and photographed after washing and air drying.

2.5. Flow cytometry analysis

A2780 cells were seeded in six-well plates, allowed to attach for 24 h and exposed to different media for 24 h. Then, the cells were harvested to prepare cell suspensions. The cells were stained with PI according to the instructions of the Cell Cycle Analysis Kit (KeyGEN, Jiangsu, China). Apoptosis was assessed according to the instructions of the Annexin V-FITC/PI apoptosis detection kit (KeyGEN, Jiangsu, China). The expression of both were analyzed by flow cytometry (Becton, Dickinson and Company, VT).

2.6. EdU staining assay

A2780 cells were treated with different concentrations of triptonide for 24 h after they were seeded in 96-well plates at a density of 5000 cells per well. EdU staining was subsequently performed to detect cell proliferation activity using a KitkFluor555 Click-iT EdU Kit (KeyGEN, Jiangsu, China) according to the manufacturer's instructions. The number of fluorescent dots represents the cell proliferation efficiency.

2.7. Quantitative real-time polymerase chain reaction (qRT–PCR)

Total RNA was extracted from cultured cells using TRIzol reagent (Invitrogen, CA, USA) and reverse-transcribed using a cDNA reverse transcription kit. (Vazyme Biotech, Nanjing, China). qPCR assays were performed with ChamQ SYBR Color qPCR Master Mix (Vazyme Biotech, Nanjing, China). The sequences of the PCR primers used were as follows: p53-Forward: 5'-CAGCACATGACGGAGGTTGT-3', reverse: 5'-TCATCCAAATACTCCACACGC-3'; 18S-Forward: 5'-GTAACCCGTTGAACCCCATT-3', reverse: 5'-CCATCCAATCGGTAGTAGCG-3'.

2.8. siRNA transfection

P53 siRNA was purchased from GenePharma (Jiangsu, China).

Cells were transfected with P53 siRNA plasmids using Lipofectamine 2000 reagent (Invitrogen) and Opti-MEM (Gibco). The experiment was conducted in three groups. The sequences of the P53 siRNA primers used were as follows:

si-P53 (sequence 1 is 5'-AAUAUUCUCCAUCCAGUGGTT-3', and sequence 2 is 5'-CACCATCCACTACAACTACAT-3'). si-Control (5'-UUCUCCGAACGUGUCACGUTT-3').

2.9. Western blot analysis

After the cells were exposed to drugs for 24 h, they were homogenized in 1× RIPA buffer (Cell Signaling Technology, MA, USA), and the protein supernatant was separated by centrifugation at 12,000 × g for 15

min at 4°C. The protein concentrations were determined by using a BCA Protein Assay Kit (KeyGEN, Jiangsu, China). The protein samples were separated via SDS—PAGE and transferred to 0.45- and 0.22-μm PVDF membranes (Millipore, Billerica, MA, USA). After they were blocked with 5% skim milk in 1× TBST for 1 h at room temperature, the membranes were incubated with primary antibody overnight at 4°C followed by incubation with secondary antibody for 1 h at room temperature. The immunoreactive bands were visualized with a gel imaging system (Bio-Rad, CA, USA) using an enhanced chemiluminescence (ECL) kit (Bio-Rad, CA, USA) and analyzed using ImageJ software.

2.10. In vivo study

Subcutaneous injection of tumor cells was used to establish a xenograft tumor model in nude mice. Approximately $400x10^4$ A2780 ovarian cancer cells were subcutaneously inoculated in the right flanks of the BALB/6 mice. Mice were purchased from Vital River (Beijing). When the tumor size reached 100 mm^3, the mice were divided into a control group (normal saline), a low concentration of triptonide (3 mg/kg) group and a high concentration of triptonide (5 mg/kg) group. The mice were intraperitoneally injected with drugs every day to observe tumor formation, and the tumor volume was measured every 2 days. The longest diameter a and the shortest diameter b of the tumor were measured, the tumor volume V was calculated according to the Formula $a*b^2/2$, and a tumor growth curve was drawn. On the 20th day, the animals were euthanized according to experimental animal ethics, the tumors were removed and weighed, and the tumor inhibition rate was calculated. The effects of triptonide on liver, lung, and heart tissues were detected via HE staining. All experimental procedures followed the requirements of the Laboratory Animal Welfare and Ethics Committee of Jinan University (Approval No. IACUC-20230913-02).

2.11. Statistical analysis

The data were derived from 2 or 3 independent experiments and are presented as the mean ± standard deviation (SD). Student's t test and one-way ANOVA were performed to analyze the significance of the difference between two groups or among multiple groups, respectively. All the statistical analyses were performed using SPSS 16.0 and GraphPad Prism 7.0. Figures were drawn with Adobe Illustrator 2021 and FigDraw. P values < 0.05 were considered to indicate statistical significance.

3. Results

3.1 Triptonide inhibits proliferation and induces apoptosis in ovarian cancer cell lines

Ten single compounds extracted from *Tripterygium wilfordii* (tripterifordin, wilforgine, wilforine, oryhosphenic acid, triptophenolide, wilforlide A, triptolide, celastrol, demethylzeylasteral, and triptonide) were used in this study. After the A2780 cell line was exposed to different concentrations of these compounds for 48 hours, the MTT assay showed that triptonide had the greatest inhibitory effect on the A2780 cell line, with an IC50 of only 2.972 nM (Fig. 1C-D). The chemical structure is shown in Fig. 1A.

Moreover, triptonide had a better antitumor effect than other common chemotherapeutic drugs (including cisplatin, carboplatin, epirubicin, 5-Fu and oxaliplatin) in the treatment of ovarian cancer (Fig. 1B).

Annexin V-FITC/PI flow cytometry showed that the apoptosis rate of A2780 cells increased in a dose- and time-dependent manner after exposure to triptonide (Fig. 2A-B). Western blot analysis showed that treatment of A2780 cells with triptonide for 24 hours increased the levels of cleaved PARP, cleaved caspase3 and cleaved caspase9 in a dose- and time-dependent manner. However, the levels of the antiapoptotic markers Bcl-2 and Bcl-xl were decreased, which suggested that triptonide induced apoptosis in A2780 cells (Fig. 2C-D). A2780 cell viability was reduced in a dose- and time-dependent manner, as detected by MTT assay after treatment with triptonide (Fig. 2F). The number of cell colonies formed in the colony formation assay (Fig. 2E) and the number of positive cells in the EdU assay were significantly reduced with increasing triptonide concentration (Fig. 2F). These findings suggest that triptonide inhibits the proliferation of A2780 cells.

3.2 Triptonide induced cell apoptosis through activating the p38/p53 pathway

To further investigate the mechanism by which triptonide induces apoptosis in A2780 cells, Western blot analysis was performed, and the results showed that the phosphorylation of the p38 and p53 proteins increased after A2780 cells were exposed to triptonide for 24 hours (Fig. 3A). Previous studies have confirmed that triggering the activation of p53 signaling via p38 causes cell apoptosis [15]. Therefore, we hypothesized that triptonide induces cell death in A2789 cells by activating p38 and phosphorylating p53 and its downstream pathways. For further verification, we added the p38 inhibitor SB203580 to the experiment. MTT assays showed that triptonide alone could inhibit the survival of A2780 cells better than the combination of SB203580 and triptonide (Fig. 3B). EdU and colony formation assays also suggested that SB203580 combined with triptonide could reverse the inhibition of cell proliferation caused by triptonide (Fig. 3C-D). Annexin V-FITC/PI flow cytometry showed that inhibition of p38 by SB203580 reversed the triptonide-induced increase in the cell apoptosis rate (Fig. 3E). Western blot analysis also showed that the expression of p38 increased in response to treatment with triptonide but was suppressed by treatment with SB203580 (Fig. 6C).

Then, we used two different p53 siRNA sequences to knock down the expression of the TP53 gene in A2780 cells, and qRT—PCR experiments showed that both p53 siRNA sequences effectively inhibited p53 gene expression (Fig. 4B). After pretreatment with p53 siRNA and subsequent treatment with triptonide, the survival rate of A2780 cells was restored (Fig. 4A), and the level of apoptosis induced by triptonide was also significantly decreased (Fig. 4D). EdU assays also suggested that p53 siRNA combined with triptonide could reverse the inhibition of cell proliferation caused by triptonide (Fig. 4C). These findings verify that triptonide inhibits the apoptosis and proliferation of A2780 cells by activating the p38/p53 pathway.

3.3 Triptonide induces apoptosis by activating autophagic death

In addition, we found that triptonide reduced p62 expression and increased LC3II and cleaved PARP levels in A2780 cells as the triptonide concentration increased gradually, but these changes were also reversed by treatment with the autophagy inhibitor bafilomycin A1 (Fig. 5A-B). These findings suggested that autophagy is activated in A2780 cells in response to triptonide. To further explore the effect of autophagy activation on A2780 cells, an MTT assay was performed, which indicated that pretreatment with bafilomycin A1 reduced the damaging effect of triptonide on cell viability (Fig. 5C). Annexin V-FITC/PI flow cytometry also demonstrated that, compared with treatment with triptonide alone, treatment with triptonide combined with bafilomycin A1 reduced cell apoptosis (Fig. 5E). The inhibition of cell proliferation in the EdU assay was also reversed by bafilomycin A1 (Fig. 5D). These findings imply that autophagy activated by triptonide is a lethal process that promotes A2780 cell death, while blocking this autophagy keeps the cells alive.

3.4 Triptonide induced S-phase arrest in A2780 cells via p38

The effect of triptonide on the physiological function of A2780 cells was further studied. Cell cycle analysis was performed by flow cytometry with PI staining. The results showed that the proportion of A2780 cells in S phase was significantly increased in a concentration-dependent manner, the proportion of cells in G2/M phase was decreased, and the proportion of cells in G1 phase was almost unchanged (Fig. 6A). In addition, the expression levels of cell cycle-related proteins measured by Western blotting showed that the S phase-related proteins Cyclin E1, Cyclin B1 and CDK2 increased with increasing triptonide concentration (Fig. 6B), which indicated that A2780 cells undergo S phase arrest after treatment with triptonide. Moreover, we speculate that this block is likely related to the p38 MAPK pathway because Sun et al. reported that the activation of p38 MAPK can cause cell cycle arrest in the S phase and inhibit cell proliferation [16]. The proportion of cells in S phase induced by triptonide was decreased, and this increase was reversed by the addition of the p38 inhibitor SB203580 (Fig. 6D). The corresponding Western blot results also showed that the S-phase protein Cyclin A2 was also reduced after SB203580 intervention (Fig. 6C). These findings demonstrated that triptonide induced S phase arrest in A2780 cells by activating p38.

3.5 Triptonide inhibits tumor growth in a xenograft tumor model

To verify the antitumor effect of triptonide in vivo, subcutaneous xenograft tumor experiments were performed in mice. Compared with that in the control group (injection of normal saline), continuous intraperitoneal injection of triptonide at different concentrations (3 or 5 mg/kg) for 20 days significantly inhibited tumor growth. There was a significantly smaller tumor volume (Fig. 7A-C) and significantly higher tumor weight (Fig. 7E) in the treated group than in the control group. Moreover, the overall body weight of mice treated with triptonide was not significantly lower than that of the control mice (Fig. 7D).

Microscopic observation of vital organs, such as the heart, liver, spleen and lung, after HE staining found no significant differences between the triptonide treatment group and the control group (Fig. 7F). These results indicate that triptonide can effectively inhibit A2780 xenograft tumors in vivo but without obvious side effects.

4 Discussion

Ovarian cancer is a common cause of death related to gynecological cancer. Approximately 60% of patients with ovarian cancer have abdominal metastasis when they are diagnosed, and these patients may lose the opportunity for surgical treatment; therefore, ovarian cancer treatment relies on chemotherapy. Although 80% of ovarian cancer patients respond well to initial treatment with commonly used platinum drugs, almost all patients experience tumor recurrence, the disease-free survival interval becomes increasingly shorter, and eventually, the tumor will gradually lose sensitivity to platinum drugs [17]. In response to the treatment of ovarian cancer, we screened triptonide from 10 monomers of *Tripterygium wilfordii* and found that it strongly inhibited the proliferation of human ovarian cancer A2780 cells in a dose-dependent manner and inhibited tumorigenesis and metastasis in vitro and in vivo. Its antitumor effect is better than that of several ovarian cancer chemotherapy drugs, such as cisplatin, carboplatin and shikonin (Fig. 1). Furthermore, the number of EdU-positive cells and colony formation in triptonide-treated A2780 cells were significantly lower, compared with those in control cells, which further confirmed the inhibitory effect of triptonide on ovarian cancer cell proliferation (Fig. 2E, 2G). Flow cytometry and Western blotting also showed that triptonide increasingly induced the apoptosis of ovarian cancer cells with increasing triptonide concentration and time (Fig. 2A-D). Mouse xenograft tumor experiments also verified the antitumor effect of triptonide in vivo, and no obvious side effects were observed (Fig. 7). Therefore, triptonide is a good drug monomer for the treatment of ovarian cancer.

The tumor suppressor protein p53 plays a key role in limiting the development of malignant tumors. Most cancers involve the loss of p53 function, which is caused by a mutation in the p53 gene itself or by a defect in the mechanism of activating p53 [18]. Moreover, p53 can mediate a series of cellular responses and activate the expression of a large variety of target genes, including apoptosis-related genes [19–22]. p53 functions primarily as a transcription factor, and overactivation of p53 leads to apoptosis and cell death [23–24]. In our study, we found that triptonide activated p53 in A2780 cells, resulting in an increase in p53 and p53 protein levels, which activated downstream targets or pathways to induce tumor cell apoptosis (Fig. 3A). After p53 was knocked down with siRNA, the degree of apoptosis was decreased, and the cell viability was restored, which suggested that triptonide promoted the apoptosis of A2780 cells by activating p53 (Fig. 4).

p38 is an important member of the mitogen-activated protein kinase (MAPK) signaling pathway. As shown in a previous study, activated p38MAPK can phosphorylate and activate many downstream effectors, including the p53 protein. The upregulation of p38 phosphorylation can activate p53 pathway-mediated apoptosis [25, 32–33]. In our study, we found that the phosphorylation of the p38 protein was increased in A2780 cells after treatment with triptonide, indicating that the p38MAPK signaling pathway

was activated (Fig. 3A). The downstream p53 protein was also activated, leading to tumor cell apoptosis. We also found that the triptonide-induced increase in apoptosis was reversed by the p38 inhibitor SB203580 or by the p53 siRNA (Fig. 3B-E, 4C-D). These findings further confirmed that triptonide promoted the apoptosis of A2780 cells through the p38/p53 signaling pathway. In addition, triptonide significantly increased the proportion of S-phase cells, decreased the proportion of G2-phase cells, and upregulated the expression of the S-phase proteins Cyclin E1 and CDK2 in A2780 cells (Fig. 6A-B). These findings indicated that triptonide caused S phase arrest in A2780 cells and that this cell cycle disruption could be reversed by SB203580, which indicated that S phase arrest was also induced through the activation of p38MAPK (Fig. 6C-D).

Autophagy is a basic physiological process in cells that is usually activated when cells are subjected to environmental stresses such as hypoxia, malnutrition, chemicals, and radiation [26–27]. Although autophagy is commonly used to recycle cellular components and maintain cellular homeostasis. Autophagy can function in a beneficial manner but can also lead to the destruction of cells [28–29]. In response to most forms of cellular stress, autophagy plays a cytoprotective role; however, in some cases of uncontrolled autophagy, upregulation of autophagy can lead to cell death or apoptosis, which may be due to activation of apoptosis or massive degradation of cell contents [30–32]. In the present study, we found that triptonide treatment induced apoptosis in A2780 cells, which was accompanied by decreased P62 and increased LC3-II levels, suggesting that autophagy was activated and that this activation led to apoptosis in A2780 cells (Fig. 5A). Triptonide-induced apoptosis was reversed by the autophagy inhibitor bafilomycin A1, further confirming that triptonide activates lethal autophagy (Fig. 5B-E). These results suggest that triptonide induces apoptosis by activating autophagy in A2780 cells.

5. Conclusions

We found that triptonide significantly inhibited the growth of A2780 tumor cells, and the MTT assay showed that triptonide, which had an IC50 of only 2.972 nM, was superior to clinical first-line chemotherapy drugs for ovarian cancer. In this study, we demonstrated that triptonide induced apoptosis in ovarian cancer cells through activation of the p38/p53 pathway and it also induced cell cycle arrest at the S phase. In addition, we found that triptonide could activate lethal autophagy, which led to growth inhibition and cell death in ovarian cancer cells, resulting in an anti-ovarian cancer effect (Fig. 8). Our findings provide a new drug candidate and strategy for the treatment of ovarian cancer.

Declarations

Author Contribution

RuoxuanLou, Taohua Yang and Xiaoying Zhang contributed equally.Both Jianwei Jiang and Yuanhong Chen are Corresponding authors.

Declaration of Competing Interests: The authors declare that they have no known competing financial interests or personal relationships that could have appeared to influence the work reported in this paper.

Funding Declaration: This research was supported by the Natural Science Foundation of Guangdong Province in China (No. 2021A1515012521), the Social Development Science and Technology Project in Dongguan city (20221800905512), the Scientific Research Project of the Traditional Chinese Medicine Bureau of Guangdong Province (20212046, 20241247), and the Science and Technology Project of Panyu District, Guangzhou (2023-Z04-001).

Data Availability Declaration The authors confirm that the data supporting the findings of this study are available within the article.

Acknowledgments: We thank the Biochemical Laboratory of Jinan University for space and the Central Laboratory of Jinan University for providing us with necessary experimental support by supplying us with a flow cytometer and an inverted fluorescence microscope. Additionally, we thank the FigDraw drawing tool.

References

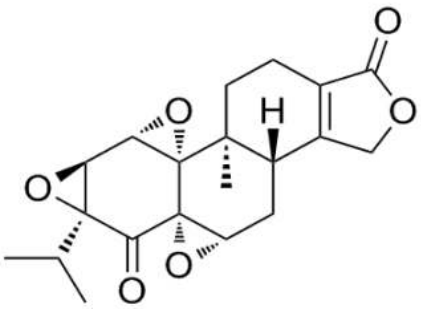
1. Stewart C, Ralyea C, Lockwood S (2019) Ovarian Cancer: An Integrated Review. Semin Oncol Nurs 35(2):151–156. 10.1016/j.soncn.2019.02.001
2. Kujawa KA, Lisowska KM (2015) Rak jajnika–od biologii do kliniki [Ovarian cancer–from biology to clinic]. Postepy Hig Med Dosw (Online) 69:1275–1290 Published 2015 Dec 2. 10.5604/17322693.1184451
3. Cho KR, Shih IM (2009) Ovarian cancer. Annu Rev Pathol 4:287–313. 10.1146/annurev.pathol.4.110807.092246
4. Gossé F, Guyot S, Roussi S et al (2005) Chemopreventive properties of apple procyanidins on human colon cancer-derived metastatic SW620 cells and in a rat model of colon carcinogenesis. Carcinogenesis 26(7):1291–1295. 10.1093/carcin/bgi074
5. Dai X, Yin C, Zhang Y et al (2018) Osthole inhibits triple negative breast cancer cells by suppressing STAT3. J Exp Clin Cancer Res. ;37(1):322. Published 2018 Dec 22. 10.1186/s13046-018-0992-z
6. Peng A, Li R, Hu J et al (2008) Flow rate gradient high-speed counter-current chromatography separation of five diterpenoids from Triperygium wilfordii and scale-up. J Chromatogr A 1200(2):129–135. 10.1016/j.chroma.2008.05.041
7. Li XX, Du FY, Liu HX, Ji JB, Xing J (2015) Investigation of the active components in Tripterygium wilfordii leading to its acute hepatotoxicty and nephrotoxicity. J Ethnopharmacol 162:238–243. 10.1016/j.jep.2015.01.004
8. Wang SS, Lv Y, Xu XC et al (2019) Triptonide inhibits human nasopharyngeal carcinoma cell growth via disrupting Lnc-RNA THOR-IGF2BP1 signaling. Cancer Lett 443:13–24. 10.1016/j.canlet.2018.11.028

9. Zhang M, Tan S, Yu D et al (2019) Triptonide inhibits lung cancer cell tumorigenicity by selectively attenuating the Shh-Gli1 signaling pathway. Toxicol Appl Pharmacol 365:1–8. 10.1016/j.taap.2019.01.002
10. Chang Z, Qin W, Zheng H et al (2021) Triptonide is a reversible non-hormonal male contraceptive agent in mice and non-human primates. Nat Commun 12(1):1253 Published 2021 Feb 23. 10.1038/s41467-021-21517-5
11. Dong F, Yang P, Wang R et al (2019) Triptonide acts as a novel antiprostate cancer agent mainly through inhibition of mTOR signaling pathway. Prostate 79(11):1284–1293. 10.1002/pros.23834
12. Vogelstein B, Lane D, Levine AJ (2000) Surfing the p53 network. Nature 408(6810):307–310. 10.1038/35042675
13. Vousden KH (2006) Outcomes of p53 activation–spoilt for choice. J Cell Sci 119(Pt 24):5015–5020. 10.1242/jcs.03293
14. Duffy MJ, Synnott NC, Crown J (2017) Mutant p53 as a target for cancer treatment. Eur J Cancer 83:258–265. 10.1016/j.ejca.2017.06.023
15. Liu RX, Ma Y, Hu XL et al (2018) Anticancer effects of oridonin on colon cancer are mediated via BMP7/p38 MAPK/p53 signaling. Int J Oncol 53(5):2091–2101. 10.3892/ijo.2018.4527
16. Sun Y, Tang S, Jin X, Zhang C, Zhao W, Xiao X (2013) Involvement of the p38 MAPK signaling pathway in S-phase cell-cycle arrest induced by Furazolidone in human hepatoma G2 cells. J Appl Toxicol 33(12):1500–1505. 10.1002/jat.2829
17. Holmes D (2015) Ovarian cancer: beyond resistance. Nature 527(7579):S217. 10.1038/527S217a
18. Olivier M, Petitjean A, Marcel V et al (2009) Recent advances in p53 research: an interdisciplinary perspective. Cancer Gene Ther 16(1):1–12. 10.1038/cgt.2008.69
19. Reinhardt HC, Schumacher B (2012) The p53 network: cellular and systemic DNA damage responses in aging and cancer. Trends Genet 28(3):128–136. 10.1016/j.tig.2011.12.002
20. Olivier M, Petitjean A, Marcel V et al (2009) Recent advances in p53 research: an interdisciplinary perspective. Cancer Gene Ther 16(1):1–12. 10.1038/cgt.2008.69
21. Vousden KH, Lu X (2002) Live or let die: the cell's response to p53. Nat Rev Cancer 2(8):594–604. 10.1038/nrc864
22. Levesque AA, Kohn EA, Bresnick E, Eastman A (2005) Distinct roles for p53 transactivation and repression in preventing UCN-01-mediated abrogation of DNA damage-induced arrest at S and G2 cell cycle checkpoints. Oncogene 24(23):3786–3796. 10.1038/sj.onc.1208451
23. Wang X, Simpson ER, Brown KA (2016) p53: Protection against Tumor Growth beyond Effects on Cell Cycle and Apoptosis [published correction appears in Cancer Res. ;76(6):1668]. Cancer Res. 2015;75(23):5001–5007. 10.1158/0008-5472.CAN-15-0563
24. Gottlieb TM, Oren M (1998) p53 and apoptosis. Semin Cancer Biol 8(5):359–368. 10.1006/scbi.1998.0098

25. García-Cano J, Roche O, Cimas FJ et al (2016) p38MAPK and Chemotherapy: We Always Need to Hear Both Sides of the Story. Front Cell Dev Biol 4:69 Published 2016 Jun 30. 10.3389/fcell.2016.00069
26. Kuma A, Mizushima N (2010) Physiological role of autophagy as an intracellular recycling system: with an emphasis on nutrient metabolism. Semin Cell Dev Biol 21(7):683–690. 10.1016/j.semcdb.2010.03.002
27. Mizushima N, Levine B (2010) Autophagy in mammalian development and differentiation. Nat Cell Biol 12(9):823–830. 10.1038/ncb0910-823
28. D'Arcy MS (2019) Cell death: a review of the major forms of apoptosis, necrosis and autophagy. Cell Biol Int 43(6):582–592. 10.1002/cbin.11137
29. Mizushima N, Levine B, Cuervo AM, Klionsky DJ (2008) Autophagy fights disease through cellular self-digestion. Nature 451(7182):1069–1075. 10.1038/nature06639
30. Maiuri MC, Zalckvar E, Kimchi A, Kroemer G (2007) Self-eating and self-killing: crosstalk between autophagy and apoptosis. Nat Rev Mol Cell Biol 8(9):741–752. 10.1038/nrm2239
31. Levine B, Yuan J (2006) Autophagy in cell death: an innocent convict? [published correction appears in J Clin Invest. ;116(12):3293]. J Clin Invest. 2005;115(10):2679–2688. 10.1172/JCI26390
32. Scott RC, Juhász G, Neufeld TP (2007) Direct induction of autophagy by Atg1 inhibits cell growth and induces apoptotic cell death. Curr Biol 17(1):1–11. 10.1016/j.cub.2006.10.053
33. Liu RX, Ma Y, Hu XL et al (2018) Anticancer effects of oridonin on colon cancer are mediated via BMP7/p38 MAPK/p53 signaling. Int J Oncol 53(5):2091–2101. 10.3892/ijo.2018.4527
34. Gan L, Wang J, Xu H, Yang X (2011) Resistance to docetaxel-induced apoptosis in prostate cancer cells by p38/p53/p21 signaling. Prostate 71(11):1158–1166. 10.1002/pros.21331

Figures

A

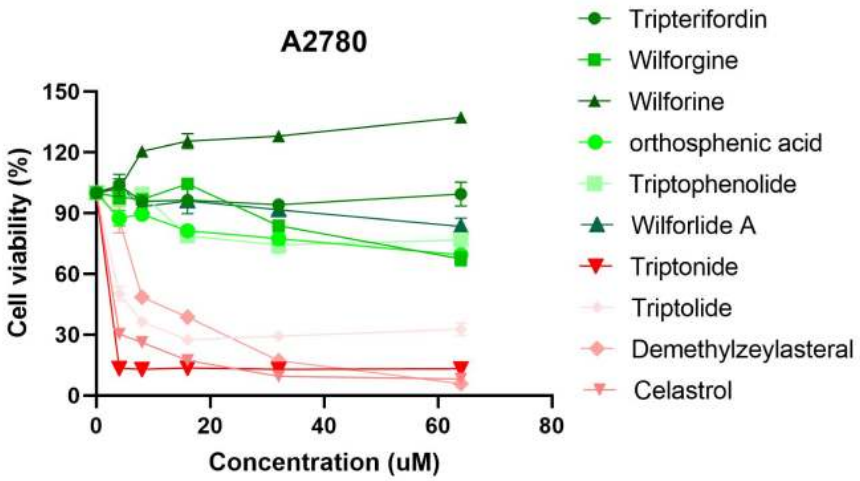


Triptonide

B

Name	IC50
Triptonide	2.972 nM
Cisplatin	10.97 μM
Carbonplatin	303 μM
5-FU	3.932 μM
Epirubicin	1.277 μM
Oxaliplatin	27.56 μM

C



D

Name	IC50
Wilforgine	>60 μM
Triptophenolide	>60 μM
Wilforlide A	>60 μM
Tripterifordin	>60 μM
Wilforine	>60 μM
Orthosphenic acid	>60 μM
Demethylzeylasteral	10.11 μM
Triptolide	1.827 μM
Celastrol	1.574 μM
Triptonide	2.972 nM

Figure 1

Comparison of the anti-ovarian cancer effects of Tripterygium wilfordii monomers and other chemotherapeutic drugs (A) Structure of triptonide (TN; www.medchemexpress.cn). (B) The inhibitory concentration (IC50) of triptonide and several clinical chemotherapy drugs on A2780 cells was detected by MTT assays. (C) A2780 cells were treated with different monomers of Tripterygium wilfordii at various concentrations for 48 h, after which cell viability was determined via MTT assays. (D) The IC50s of different monomers of Tripterygium wilfordii toward A2780 cells. The data shown are presented as the means ± SDs and were confirmed in three separate experiments.

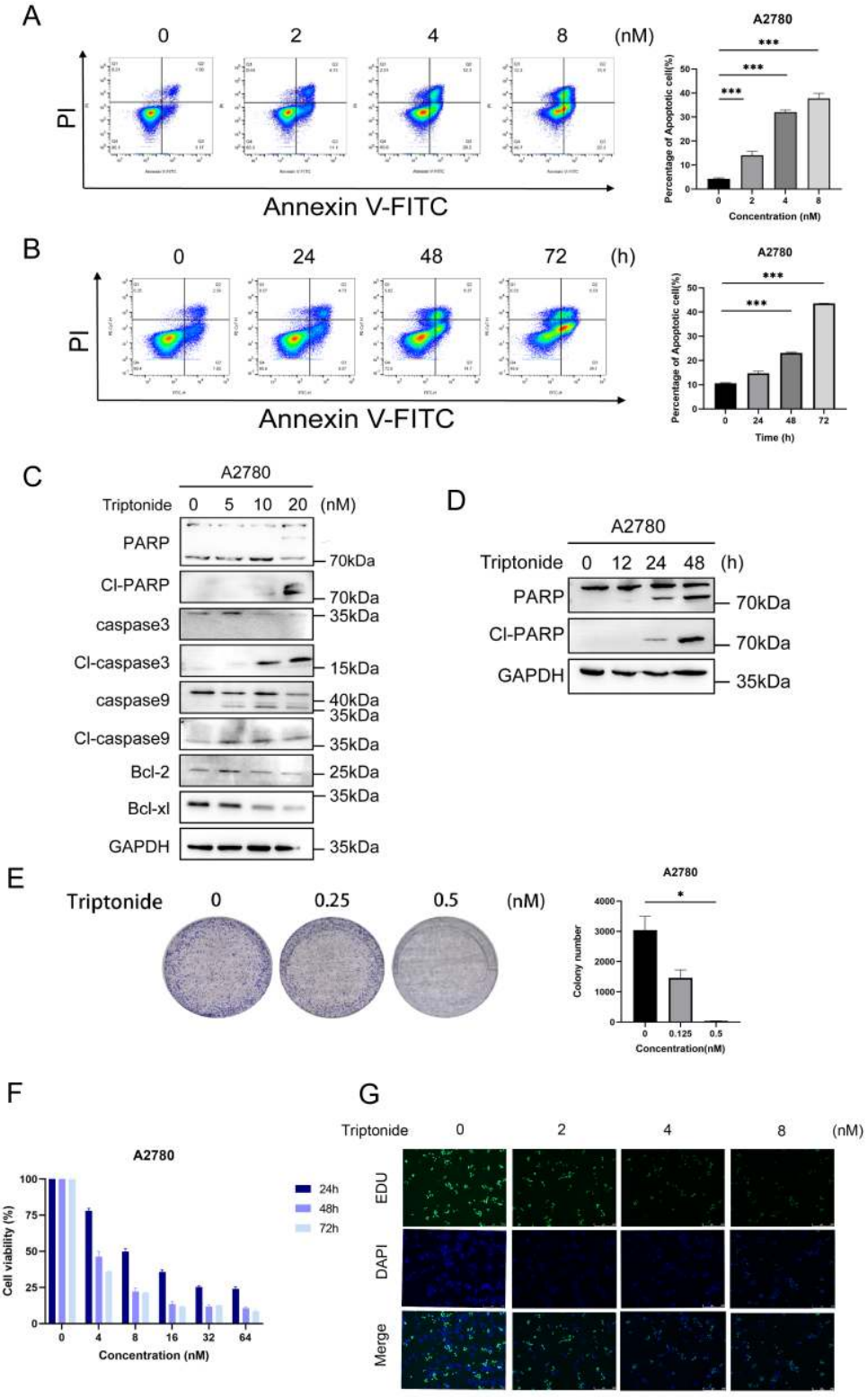


Figure 2

Triptonide inhibited the proliferation of human A2780 cells in a dose- and time-dependent manner. (A) A2780 cells were treated with different concentrations of TN for 24 h, and cell apoptosis was assessed quantitatively by Annexin V/PI flow cytometry analysis. (B) A2780 cells were treated with 2 nM TN for 0-72 h, and cell apoptosis was assessed quantitatively by Annexin V/PI flow cytometry analysis.

(C) (D) Western blot analysis showing the effects of TN treatment on apoptosis markers in A2780 cells. (E) A2780 cells were evaluated through a colony formation assay after treatment with different concentrations of TN for 14 days. (F) A2780 cell viability was measured by MTT assay after treatment with different concentrations of TN for 24, 48 and 72 hours. (G) Inhibition of proliferation was analyzed by an EdU staining assay after A2780 cells were treated with different concentrations of TN for 24 h. The number of fluorescent dots represents the cell proliferation efficiency. Representative data from one of three independent experiments are shown. The data are presented as the mean ± SD. *p < 0.05, ** p < 0.01, *** p < 0.001.

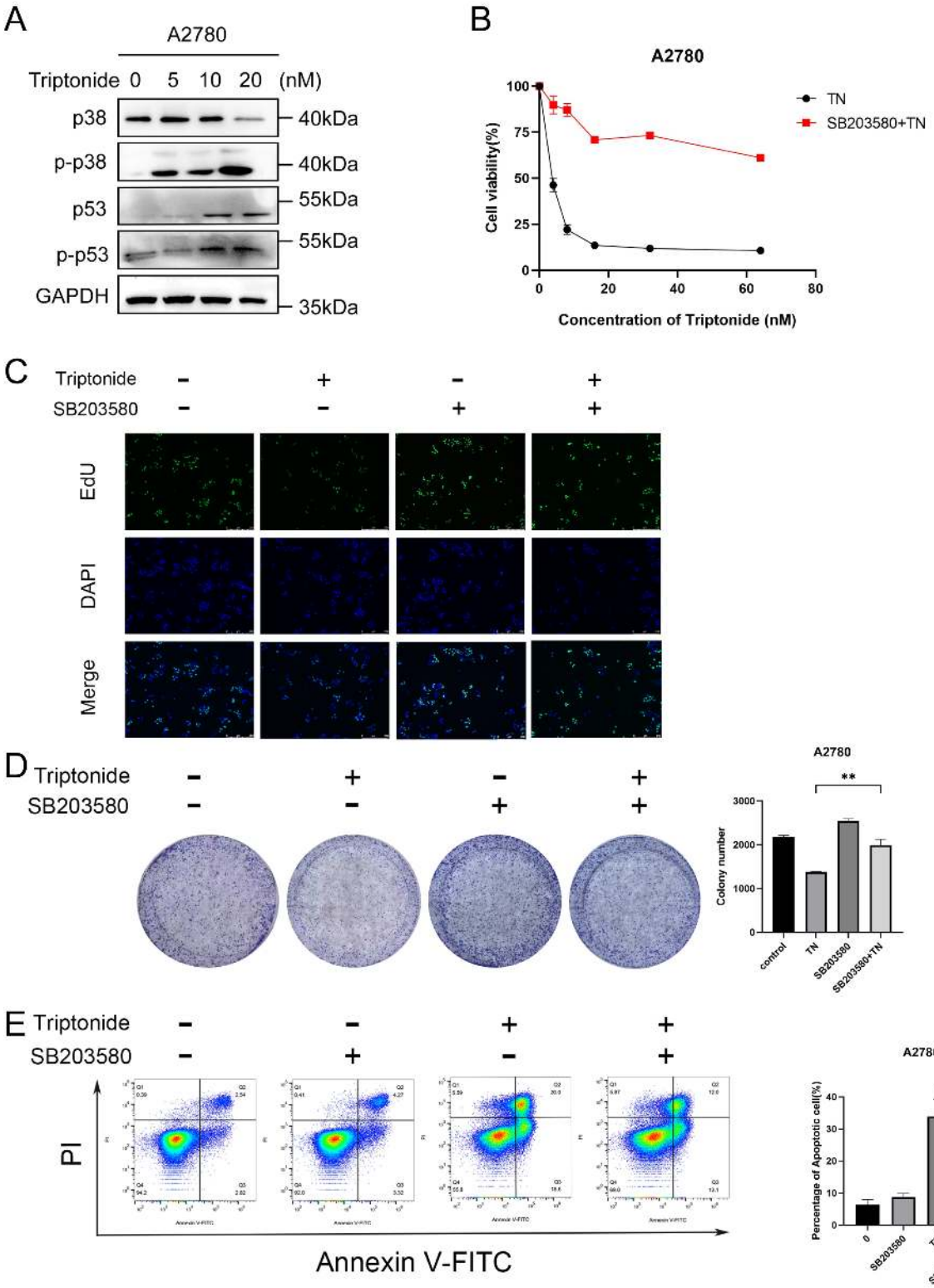


Figure 3

Triptonide induces apoptosis and inhibits the proliferation of A2780 cells by activating the p38 pathway (A) Western blot analysis identified p53 and p38 protein markers in A2780 cells treated with different concentrations of TN for 24 h. (B) A2780 cell viability was measured by MTT assay after treatment with different concentrations of TN alone or in combination with 15 μM SB203580. (C) Inhibition of proliferation was analyzed by an EdU staining assay after treatment with 4 nM TN and/or 15 μM

SB203580. (D) Colony formation assay after A2780 cells were treated with 0.25 nM TN and/or 15 μM SB203580 for 14 days. (E) A2780 cell apoptosis was assessed quantitatively by Annexin V/PI flow cytometry analysis after treatment with 8 nM TN and/or 20 μM SB203580. Representative data from one of three independent experiments are shown. The data are presented as the mean ± SD. ** p < 0.01, *** p < 0.001.

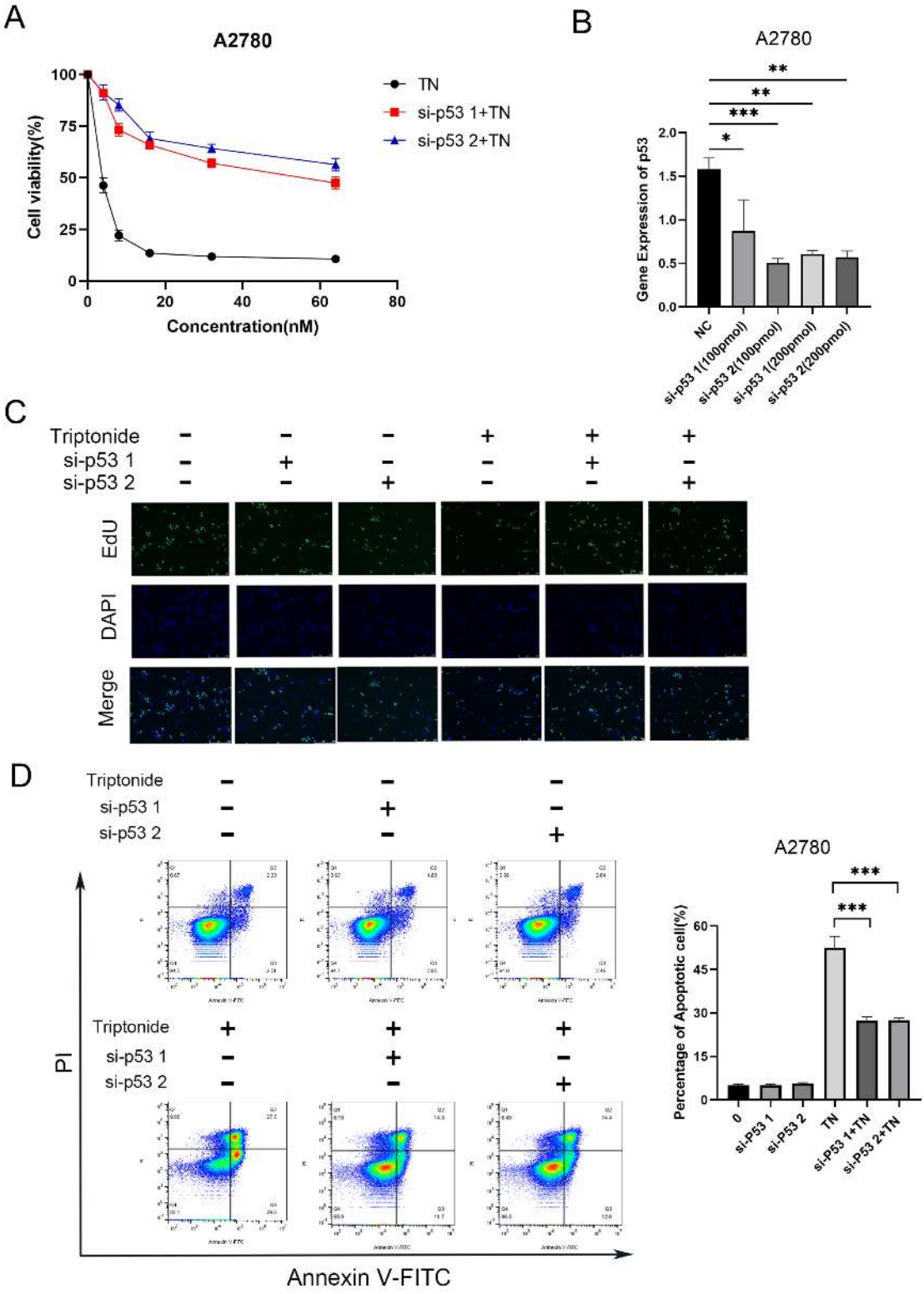


Figure 4

Triptonide induced apoptosis by activating p53 in A2780 cells. (A) A2780 cell viability was measured by MTT assay after treatment with different concentrations of TN alone or with TN combined with p53 siRNA for 48 hours. (B) qRT–PCR was used to determine whether p53 siRNA inhibited the gene expression of TP53 in A2780 cells. (C) Inhibition of proliferation was analyzed by an EdU staining assay after A2780 cells were treated with 4 nM TN and/or p53 siRNA for 48 hours. (D) A2780 cells were treated with 4 nM TN and/or p53 siRNA (100 pmol) for 24 h, and cell apoptosis was assessed quantitatively by Annexin V/PI flow cytometry analysis. Representative data from one of three independent experiments are shown. The data are presented as the mean ± SD. ** $p < 0.01$, *** $p < 0.001$.

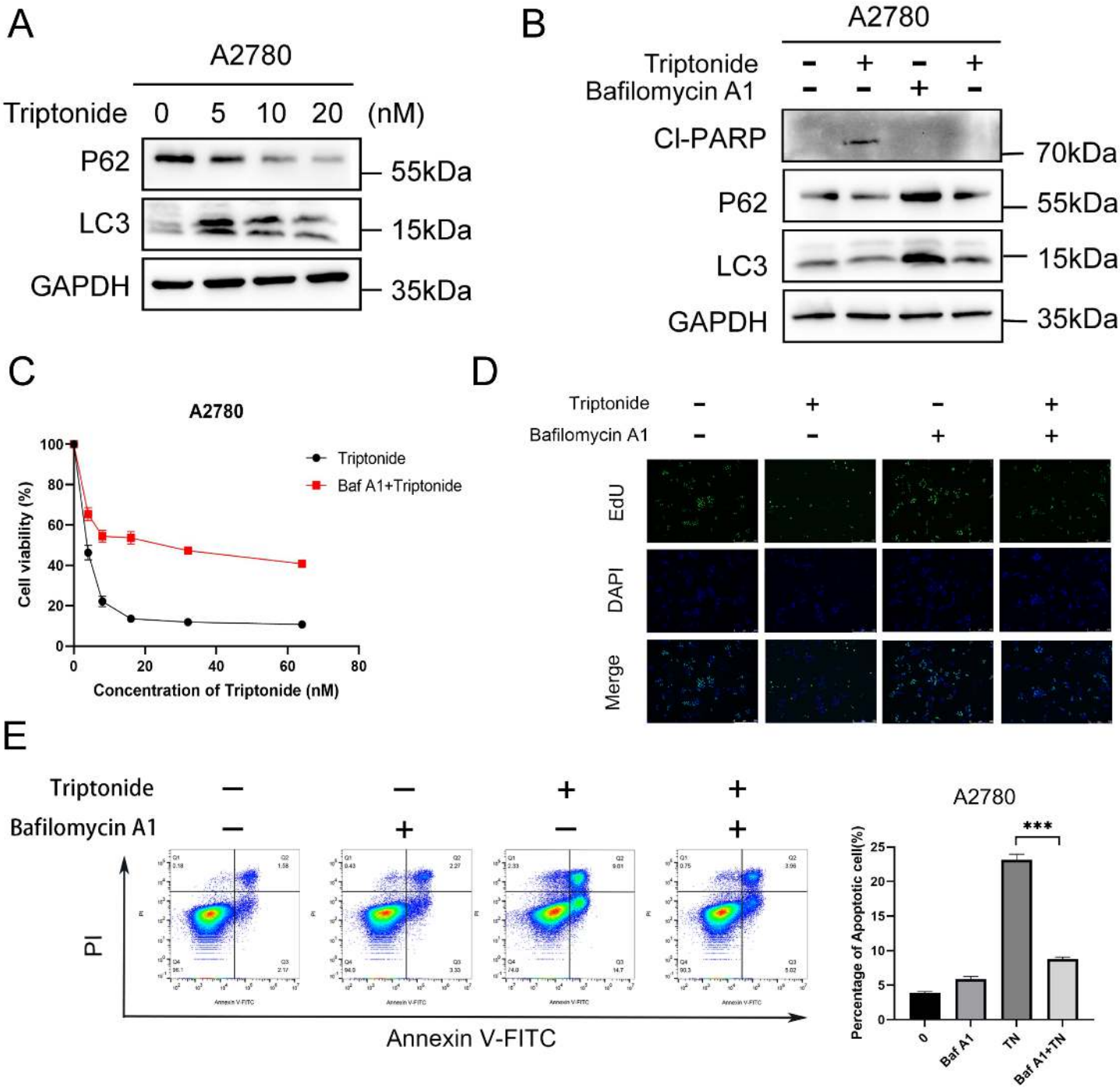


Figure 5

Triptonide induces lethal autophagy in A2780 cells. (A) (B) Western blot analysis of autophagy-related protein markers in A2780 cells treated with 10 nM TN and/or 800 nM bafilomycin A1 for 24 h. (C) A2780 cell viability was measured by MTT assay after treatment with TN alone or in combination with 250 nM bafilomycin A1 for 48 hours. (D) Inhibition of proliferation was analyzed by an EdU staining assay after treatment with 4 nM TN and/or 250 nM bafilomycin A1. (E) A2780 cell apoptosis was assessed quantitatively by Annexin V/PI flow cytometry analysis after treatment with TN and/or 800 nM bafilomycin A1 for 24 hours. Representative data from one of three independent experiments are shown. The data are presented as the mean ± SD. ** p < 0.01, *** p < 0.001.

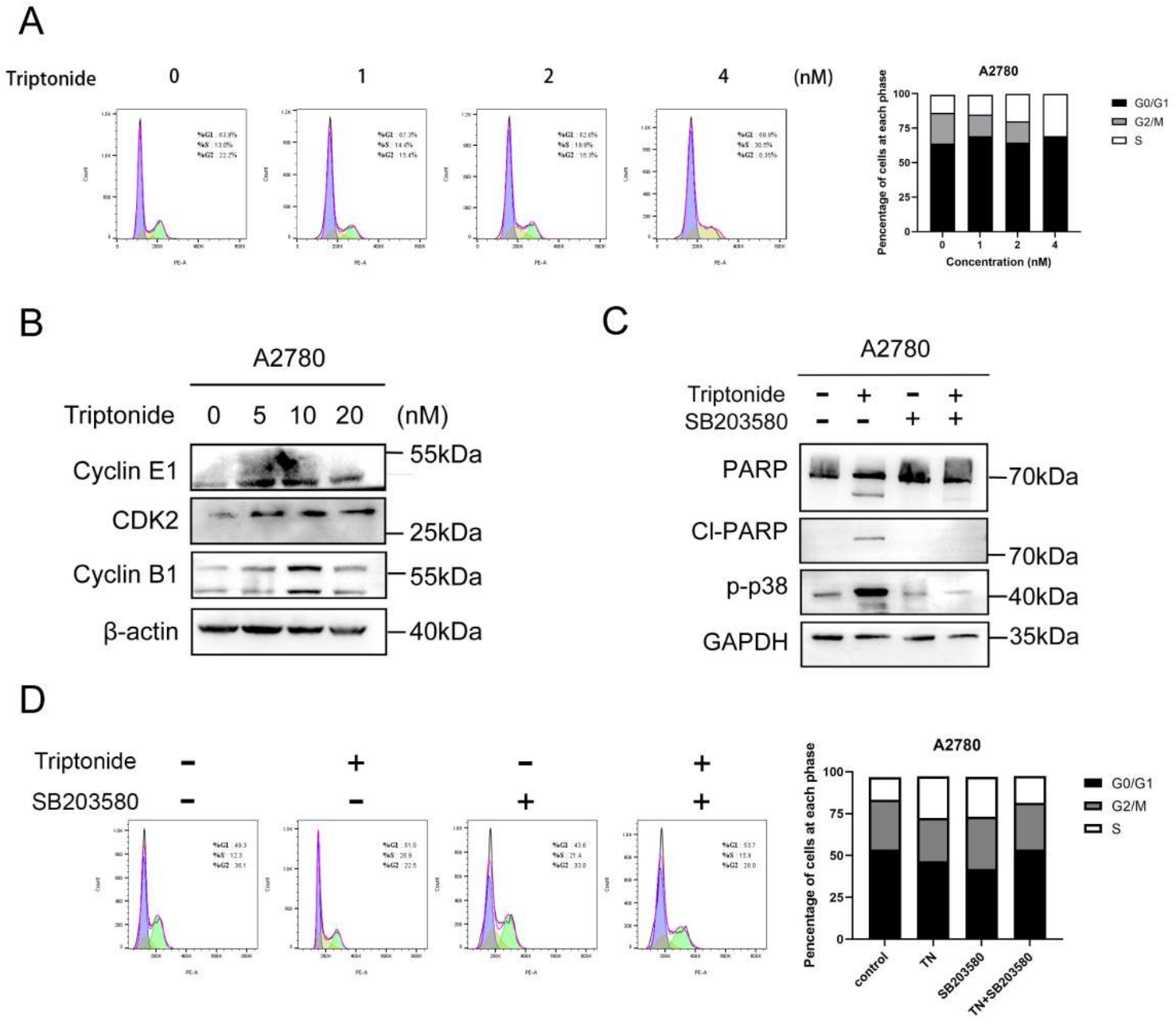


Figure 6

Triptonide induced S phase arrest by activating the p38 pathway (A) Cell cycle analysis after A2780 cells were treated with different concentrations of TN for 24 h. (B) Western blot analysis showing the effects

of A2780 cells treated with TN for 24 h on cell cycle-related protein markers. (C) Western blot analysis and cell cycle analysis after A2780 cells were treated with 10 nM TN and/or 20 μM SB203580. (D) Cell cycle analysis after A2780 cells were treated with 4 nM TN and/or 20 μM SB203580. Representative data from one of three independent experiments are shown. ** p < 0.01, *** p < 0.001.

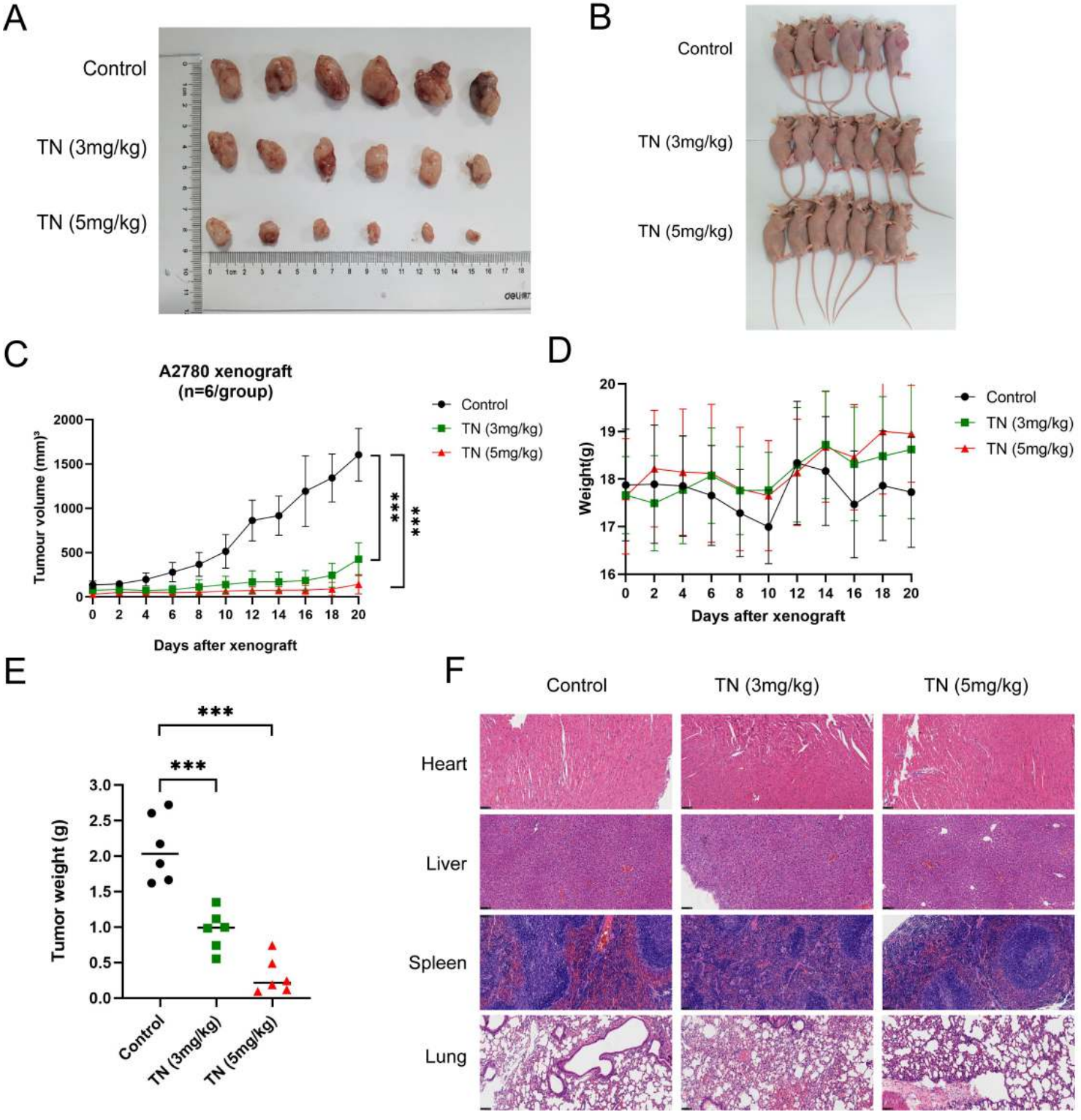


Figure 7

The antitumor effect of TN on an in vivo xenograft tumor model of ovarian cancer. (A) (B) Morphological images of A2780 xenografts after treatment with vehicle or TN at a dose of 3 or 5 mg/kg/d for 20 days. (C) Changes in tumor volume and (D) mouse body weight after treatment with vehicle or TN at a dose of 3 or 5 mg/kg/d for 20 days. (E) Tumor weight after treatment for 20 days. (F) HE staining of tissues from mice in the vehicle group and TN group at a dose of 3 or 5 mg/kg/d. Representative data from one of three independent experiments are shown. The data are presented as the mean ± SD. ** $p < 0.01$, *** $p < 0.001$.

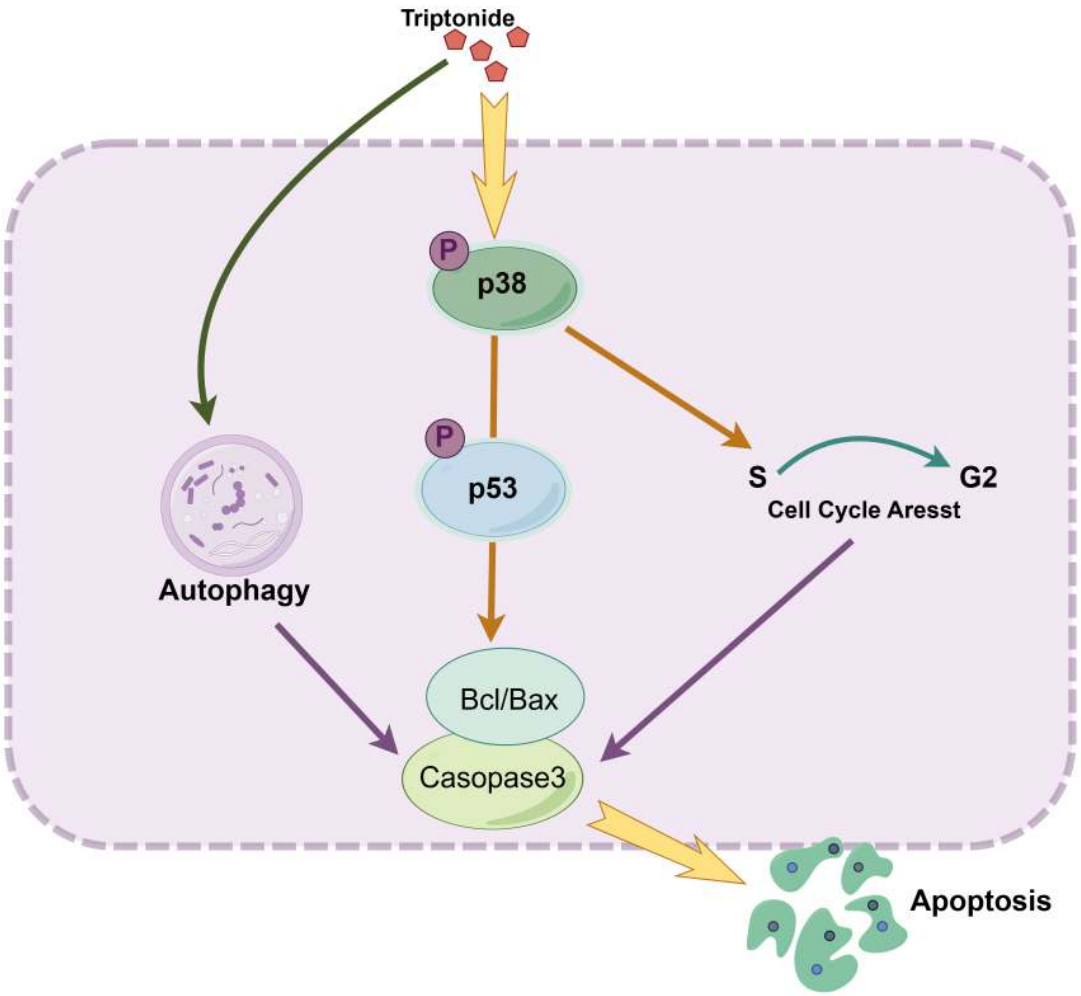


Figure 8

Diagram of the effect of triptonide on A2780 cells.